

# Dual pH-Responsive Hydrogel Actuator for Lipophilic Drug Delivery

Zilong Han, Peng Wang, Guoyong Mao, Tenghao Yin, Danming Zhong, Burebi Yiming, Xiaocheng Hu, Zheng Jia, Guodong Nian,\* Shaoxing Qu,\* and Wei Yang

Cite This: *ACS Appl. Mater. Interfaces* 2020, 12, 12010–12017

Read Online

ACCESS |

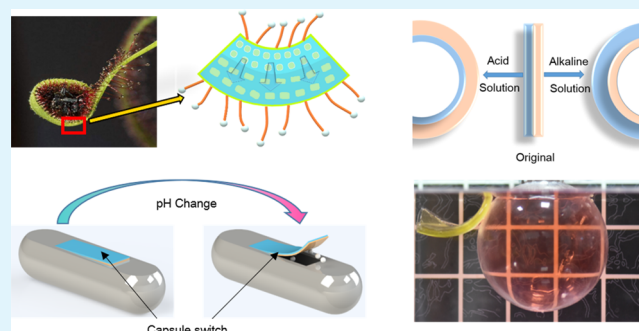
Metrics & More

Article Recommendations

Supporting Information

**ABSTRACT:** As one of the most promising drug delivery carriers, hydrogels have received considerable attention in recent years. Many previous efforts have focused on diffusion-controlled release, which allows hydrogels to load and release drugs in vitro and/or in vivo. However, it hardly applies to lipophilic drug delivery due to their poor compatibility with hydrogels. Herein, we propose a novel method for lipophilic drug release based on a dual pH-responsive hydrogel actuator. Specifically, the drug is encapsulated and can be released by a dual pH-controlled capsule switch. Inspired by the deformation mechanism of Drosera leaves, we fabricate the capsule switch with a double-layer structure that is made of two kinds of pH-responsive hydrogels. Two layers are covalently bonded together through silane coupling agents. They can bend collaboratively in a basic or acidic environment to achieve the “turn on” motion of the capsule switch. By incorporating an array of parallel elastomer stripes on one side of the hydrogel bilayer, various motions (e.g., bending, twisting, and rolling) of the hydrogel bilayer actuator were achieved. We conducted an in vitro lipophilic drug release test. The feasibility of this new drug release method is verified. We believe this dual pH-responsive actuator-controlled drug release method may shed light on the possibilities of various drug delivery systems.

**KEYWORDS:** capsule switch, actuator control, drug release, dual pH-responsive hydrogel



## INTRODUCTION

Hydrogels have gained considerable attention in recent years as one of the most promising drug delivery systems, especially for oral administration.<sup>1</sup> The extremely high water content gives hydrogels the physical similarity to the tissues, excellent biocompatibility, and capability to encapsulate hydrophilic drugs.<sup>2,3</sup> In the diffusion-controlled drug delivery system, the compatible drugs are encapsulated in hydrogel carriers, protected against denaturation and degradation, and delivered to the target by various means. This hydrogel delivery system is suitable for most hydrophilic drugs except the lipophilic drugs. Currently, more than 40% of the therapeutically active compounds are lipophilic and exhibit poor water solubility.<sup>4,5</sup> In addition, advances in modern chemical synthesis processes have led to the massive development of lipophilic drugs. Delivery of lipophilic drugs through hydrogel is challenging due to their poor compatibility with the hydrogel.<sup>6</sup> To address this problem of lipophilic drugs, various strategies have been explored. Several critical issues should be taken into account when designing hydrogels for controlled drug delivery: first, poor aqueous solubility limits the clinical use of hydrogel because lipophilic drugs may precipitate in aqueous media; second, acidic medium in the stomach may lead to the premature breakdown of certain drugs in the gastrointestinal tract (GIT); third, conventional drug administration often requires high dosages or repeated administration to stimulate a

therapeutic effect that leads to the severe side effects and even toxicity; forth, poor targeting reduces the efficacy.<sup>4,7,8</sup>

Natural actuating systems in plants inspired many previous efforts on hydrogel actuators whose bilayer structures were designed to enable reversible twisting and bending in response to stimuli such as light, temperature, moisture, and magnetic fields.<sup>9–20</sup> For example, as one kind of small insectivore, Drosera (Figure 1a) can lure, capture, and digest insects using glandular tentacles, which secrete sweet and sticky mucilage to attract and ensnare insects and are extremely sensitive. The tentacles can fold up and surround the prey over several minutes to several hours to digest the prey with secreted digestive enzymes.<sup>21,22</sup> The rapid movement of the tentacle is achieved by the synergistic effect of bilayer structure (rapid shrinking in the adaxial half of the tentacle and swelling in the abaxial half).

Choosing appropriate materials for synthetic polymer actuators to meet the specific environmental needs is critical to their potential applications in artificial muscles, soft robotics, and flexible electronics.<sup>23</sup> Different from changing the ambient

**Received:** November 30, 2019

**Accepted:** February 13, 2020

**Published:** February 13, 2020

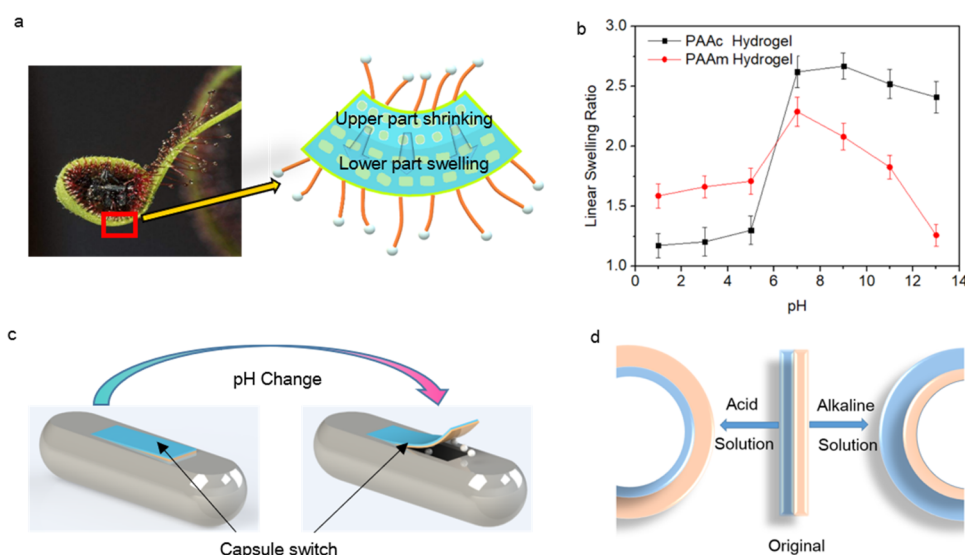


**Figure 1.** Design of the capsule switch based on a dual pH-responsive hydrogel actuator. (a) Rapid catapulting movement of the tentacle is induced by the rapid shrinking in the upper part of the tentacle but swelling in the lower part. (b) Swelling behavior of polyacrylic acid (PAAc) and polyacrylamide (PAAm) hydrogels in a series of aqueous solutions with pH values ranging from 1 to 13 at room temperature. (c) Actuator-controlled drug release model. (d) Bidirectional bending of the PAAc/PAAm hydrogel bilayer structure.

temperature or creating a specific magnetic field, regulating the pH of the surrounding aqueous solution to drive pH-sensitive hydrogel actuators is relatively facile to implement in the human body. Generally, pH-sensitive hydrogels are weak polyelectrolyte hydrogels that swell or shrink in aqueous solutions of different pH values.<sup>24,25</sup> Due to the variation of pH along the digestive tract (from pH = 2 in the stomach to 8 in the intestine), pH-sensitive hydrogels have been widely studied and used in drug delivery.<sup>26</sup> The pH-dependent ionization of basic functional groups on hydrogel chains responsible for swelling is shown in Figure S1. Figure 1b shows the distinct linear swelling ratio changes of polyacrylamide (PAAm) hydrogel and polyacrylic acid (PAAc) hydrogel with the solutions of different pH values from 1 to 13 at room temperature. These properties of hydrogels can be exploited for drug delivery. We choose PAAm hydrogel and PAAc hydrogel to fabricate the dual pH-sensitive bilayer hydrogel. In addition, to achieve tough bonding between two layers, silane coupling agents<sup>27</sup> are added to the precursors of both PAAm hydrogel and PAAc hydrogel (Figure S2). After polymerization, two hydrogels were put together for 1 day during which the coupling agents condensed, added cross-links inside the networks, and formed bonds between the networks (Figure S3; Supporting Information Methods). We measure the adhesion energy using the 90 degree peeling test (Figure S4 and Movie S1). If the coupling agents are not added, or only added to one precursor, the adhesion energy is low, and the hydrogel is peeled off. If the coupling agents are added to both precursors, the peeling test of the toughened layers gives adhesion energy of  $132 \text{ J} \cdot \text{m}^{-2}$  (calculated from Figure S5), and fracture occurs in the hydrogel (Figure S4). Even if it is soaked in an acid solution or an alkaline solution for 24 h, the interface would not de-bond.

Here, we propose a new drug release method based on a dual pH-responsive bilayer actuator. The drugs are encapsulated in a capsule and can be released by a dual pH-controlled capsule switch (Figure 1c). Inspired by the Drosera leaves, the capsule switch has a bilayer structure that is made of two kinds of pH-responsive hydrogels. The actuator is capable of

bidirectional and programmable bending achieved by collaboratively asymmetric swelling and shrinking of the cationic and anionic networks in acid or alkaline solutions (Figure 1d and Movie S2). To simulate the lipophilic payload releases, this actuator is initially adhered to the capsule and thus capable of turning on when subjected to the acidic or basic environment. Both hydrophilic and lipophilic drug delivery can be easily achieved using this method. The actuator-controlled drug release system has the advantages of drug protection and good targeting, which can not only expand the application of lipophilic drugs but also improve the loading efficiency of drugs.

## EXPERIMENTAL SECTION

**Materials.** Acrylic acid 99% (AAc, Lot number 147230), *N,N'*-methylenebisacrylamide 98% (MBAA, Lot number 146072), ammonium persulfate 98% (Lot number 248614),  $\alpha$ -ketoglutaric acid 98.5% (Lot number 75890), and 3-(trimethoxysilyl) propyl methacrylate (TMSPMA, Lot number M6514) were purchased from Sigma-Aldrich, and acrylamide 99% (AAm, Lot number A108465) was purchased from Aladdin, Shanghai, China. Very high bond (VHB) was purchased from 3 M China, Shanghai, China. All the reagents were used as received.

**Methods. Fabrication Process of the Dual pH-Sensitive Bilayer Hydrogel.** As shown in Figure S2, AAm monomers are dissolved in distilled water to form a solution of concentration 2 mol/L. For every 1 mL of the solution, 4  $\mu\text{L}$  of 0.1 mol/L MBAA is added as the cross-linker, 20  $\mu\text{L}$  of 0.1 mol/L ammonium persulfate is added as the UV initiator, and 1.9  $\mu\text{L}$  of TMSPMA is added as a coupling agent. The solution is vigorously stirred and poured into a mold made of laser-cut acrylic sheets. The mold and the solution are covered at the bottom of a thin acrylic sheet to prevent oxygen inhibition. The covered mold is then placed under a UV lamp. The mixed solution is exposed to UV irradiation ( $\lambda = 365 \text{ nm}$ ) for 60 min to prepare the PAAm layer (i.e., cationic layer). Second, the layer of PAAc hydrogel (i.e., anionic layer) is synthesized in a similar way using 2 mol/L AAc solution. Third, hydrogels are taken out from the molds and washed with deionized water thoroughly to remove all unreacted monomers. To bond them together, we stack the PAAm and PAAc hydrogel layers and keep the bilayer in a sealed Petri dish at room temperature for 1 day.

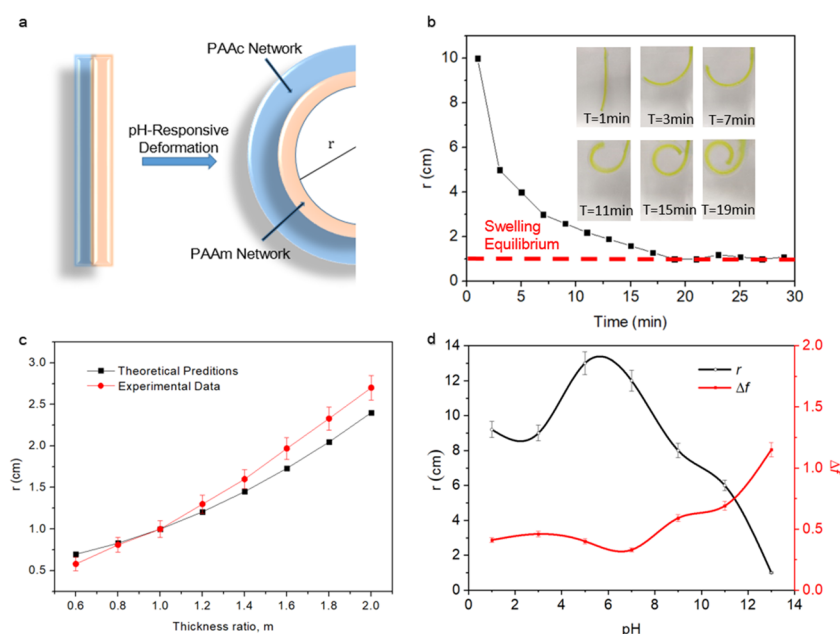


**Figure 2.** Shape transformation of the PAAm–PAAc bilayer actuator in aqueous solution. (a) Schematic of the actuator bending in an aqueous solution of a certain pH value, where  $r$  is the inner radius of the bent actuator. (b) A typical bending process of the actuator in a pH of 13 of NaOH aqueous solution. The actuator bends gradually with a decreasing radius against time, and finally reaches a minimum after 20 min. The inset shows snapshots of the actuator during bending. (c) Theoretical prediction and experimental data of the inner radius of the bent actuator versus the thickness ratio  $m$  for pH of 13. (d) Effect of solution pH on the bending performance of the actuator. The variation of  $r$  and the difference between swelling ratios of the PAAc and PAAm hydrogels  $\Delta f$  are plotted as functions of pH values.

**Measurement of Adhesion.** Both PAAm hydrogel and PAAc hydrogel are prepared as described above in the size of  $50 \times 30 \times 2 \text{ mm}^3$ . They are stacked right after curing, but a paraffin film ( $20 \times 30 \text{ mm}^2$ ) is inserted in between at one end to prevent the bonding in the corresponding area and serves as a precrack. Then, the bilayer sample is kept at room temperature for 1 day to develop the adhesion. To prevent the hydrogel from dehydration, we seal the sample in a Petri dish. After bonding formation, the bilayer structure is taken out of the Petri dish. Using a cyanoacrylate adhesive (Loctite 406, Henkel), we bond the PAAm side to a glass slide that serves as a rigid substrate in the peeling test. The PAAc side is glued to a thin nonwoven fabric film, which serves as a flexible, inextensible backing for the PAAc hydrogel. The bilayer sample with a glass substrate and nonwoven fabric backing layer is loaded to a mechanical tester (50 N load cells; Instron 5944 Single Column) using the 90 degree peeling fixture. The peeling rate is 10 mm/min. The adhesion energy is given by the plateau value of the force–displacement curve.

**pH-Sensitive Swelling Behavior.** The individual PAAc and PAAm hydrogels are cut into squares with a certain side length of  $d_i$ . The samples are thoroughly dried and then immersed in 50 mL of aqueous solutions with different pH levels for 20 min. After swelling, we blot the hydrogels with a piece of paper towel and measure the side length of the squares. The swelling ratio of the linear dimensions is defined as  $f = d_f/d_i$ , where  $d_f$  is the final side length of the hydrogel and  $d_i$  is the initial side length of the hydrogel. The pH value of the solution is regulated using HCl or NaOH solution and measured with a pH meter (PHS3C, Rex, Shanghai, China).

**Shape Transformation Tests of the Bilayer Actuator.** Samples of the PAAm hydrogel and PAAc hydrogel bilayer actuator are prepared in the size of  $100 \times 10 \times 2 \text{ mm}^3$ . The actuators bend to different degrees in aqueous solutions of different pH levels. The bending motion of the actuator in a given solution is recorded by a digital camera. The curvature of the actuators is measured using image-processing software.

**Design of Programmable Actuator.** An array of parallel thin elastomer stripes is bonded on one surface of the hydrogel layer ( $100 \times 50 \times 2 \text{ mm}^3$ ) using 502 Instant Adhesive. Then, we change the fiber

architectures with the lead angle ( $0^\circ$ ,  $45^\circ$ , and  $90^\circ$ ) of the stiff stripes relative to the long edge of the actuator.

**Lipophilic Payload Releases Simulation.** For the ease of observation and analysis, we amplified the size of the functional capsule (a 6 cm diameter polyethylene sphere) in this simulation experiment. A preset outlet ( $1 \text{ cm} \times 1 \text{ cm}$ ) of the simulation capsule is covered by the bilayer actuator ( $3 \text{ cm} \times 2 \text{ cm}$ ). The upper part of the actuator is firmly fixed, and the rest slightly adheres to the surface of the capsule with poly(vinyl alcohol) (PVA) glue. The functional capsule has good airtightness before the experiment. Then, dye solution with 0.5 g of carotenoid, which is used as the lipophilic drug model for in vitro dissolution studies, is injected into the dummy capsule. After these steps, we soaked the loaded capsules in different aqueous solution with the pH levels of 2, 6, and 8, respectively. At predetermined time intervals, volumes of 3 mL of samples are withdrawn and spectro-photometrically analyzed (UV–vis spectroscopy) at 450 nm for carotenoid. The concentration of released carotenoid is calculated by plotting the calibration curve.

## RESULTS AND DISCUSSION

**Shape Transformation in Aqueous Solutions.** The actuator's ability to transform in response to pH changes is endowed by the synergy of the PAAm and PAAc hydrogels. We adopt the Timoshenko formula that predicts the evolution of their deformation ( $r$  is the inner radius of the bent actuator shown in Figure 2a). Previously used to describe the bending behavior of a uniformly heated bilayer strip with different expansion coefficients, this formula is also suitable for the bending of bilayers made of soft materials.<sup>28–30</sup>

We assume that the curvature along the width direction of the sample is negligible. From Figure 2b, we find that the flat actuator ( $100 \text{ mm} \times 10 \text{ mm}$ , length  $\times$  width) bends gradually toward the PAAm hydrogel when soaked in an alkaline solution (pH = 13). As shown in Figure 1b, the swelling ratio of the PAAc hydrogel is higher than that of the PAAm hydrogel for a pH of 13, and this may cause nonuniform

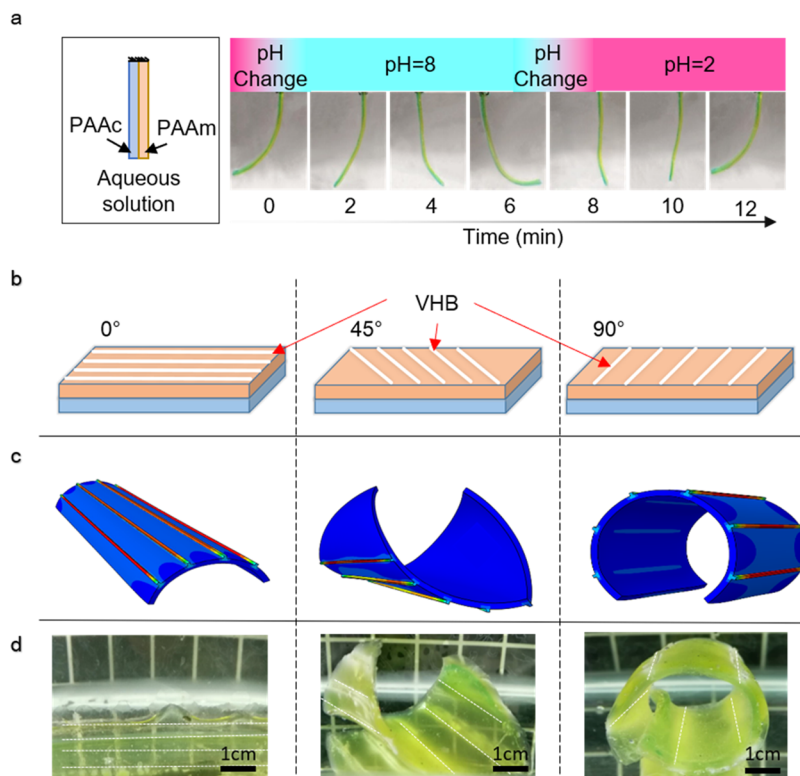


**Figure 3.** Programmable bending deformation. (a and b) Bidirectional bending actuation in different pH solutions. (a) Experimental images of the shape transformation of the actuator caused by changes in the pH values. At first, the actuator bends to the left when the pH is 2. Then, when the pH of the solution is adjusted to 8, the actuator gradually straightens and finally bends to the right. The actuator recovers to its initial state when the pH is further tuned to 2. (b) Schematic of PAAM–PAAC bilayer actuators with VHB stripes glued on one side. The VHB stripes are arranged at an angle of 0, 45, or 90° with respect to the long edge of the hydrogel. (c) Predictions by simulations for the actuators with VHB stripes. (d) Dual pH-responsive hydrogel directionally controlled actuation with the different lead angles of the stiff stripes relative to the long axis in an alkaline solution (pH 13).

internal stresses along the interface of the bilayer actuator. The swelling equilibrium of the bilayer actuator is reached after being soaked for 20 min in the alkaline solution with a constant  $r$  (10 mm). Using the Timoshenko formula, one can explain the bending behaviors of the bilayer actuator. The related equations are modified as follows

$$r \sim \frac{a_2(3(1+m)^2 + (1+mn)\left(m^2 + \frac{1}{mn}\right))}{6\Delta f(1+m)} \quad (1)$$

$$r = \frac{Ka_2(3(1+m)^2 + (1+mn)\left(m^2 + \frac{1}{mn}\right))}{6\Delta f(1+m)} \quad (2)$$

where  $r$  is the inner radius of the swelled bilayer,  $f$  is the swelling ratio in the linear dimension (i.e., the ratio of the length of the bilayer in undeformed state to that in swelling state),  $m = a_1/a_2$  is the ratio of the thickness of the PAAM layer ( $a_1$ ) to that of the PAAC layer ( $a_2$ ) in the flat state,  $n = E_{\text{PAAM}}/E_{\text{PAAC}}$  is the elastic modulus ( $E$ ) ratio (Supporting Information Figure S6),  $\Delta f$  is the difference of linear dimension ratios between the PAAC and PAAM, i.e.,  $\Delta f = f_{\text{PAAC}} - f_{\text{PAAM}}$ , and  $K$  is the compensation coefficient. According to eq 2,  $r$  can be regulated by  $a_2$ ,  $m$ ,  $n$ , and  $\Delta f$ . To verify the formula used for the bilayer actuator, we might use one experimental test to determine the evolution of  $r$  and get the compensation coefficient  $K$  under the specific pH condition. Next, we used the obtained data and eq 2 to predict the curvature evolution for other samples with the same  $a_2$ , but a different  $a_1$  value.

When soaked in an alkaline solution (e.g., pH = 13),  $r$  is found to increase with  $m$  (Figure 2c). This result agrees well with the prediction by eq 2 (Figure 2c), within the given range of  $m = 0.6$ – $2$ . The parameters are taken as  $K = 3.71$  (Table S1),  $n = 4.35$  (calculated from Supporting Information Figure S6),  $\Delta f = 1.15$ , and  $a_2 = 2$  mm. Finally, as pH affects the swelling behavior of the bilayer actuator, for an aqueous solution with a certain pH, the parameters of the bilayer actuator should be first calibrated by comparing the experimental data with the formula. As shown in Figure 1b, in a relatively high pH solution (pH > 6), the PAAC layer with numerous ionized carboxyl groups exhibited higher swelling, while the swelling ratio of the PAAM layer is much lower and decreases with pH. This results in a negative correlation between  $\Delta f$  and  $r$  (Figure 2d), which can be explained by eq 2. Therefore, the bending of the bilayer actuator can be controlled simply by the significant difference in swelling behaviors of the PAAM and PAAC layers under designated pH values.

**Direction-Controlled Bending Deformation.** As an actuator, it is very important to be able to achieve a variety of deformations to meet different needs. For example, bidirectional bending allows the pH-responsive actuator to work properly in both acidic and alkaline conditions. In addition, sometimes there is not enough space for a switch to fully open to release drugs due to the space constraints. Under the premise of ensuring that the switch can be fully opened in space-limited condition, the programmable bending is

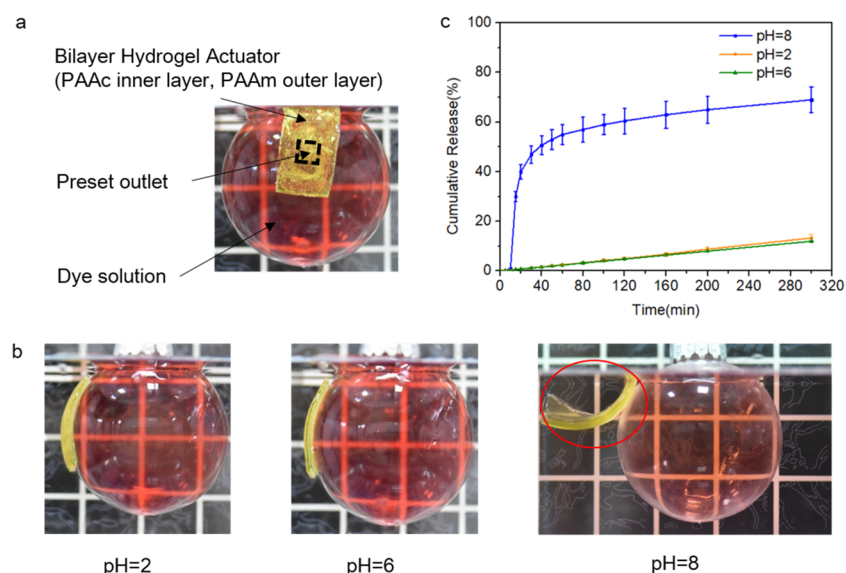


**Figure 4.** Demonstration of in vitro lipophilic drug release. (a) Amplified functional capsule model. (b) Capsules are soaked in different aqueous solutions of pH 2, 6, and 8. The capsule switch opens within 20 min in the alkaline solution (pH = 8). (c) In vitro release of carotenoid in solutions of different pH (2, 6, and 8) values in 300 min.

necessary. Attention is now focused on the capability of the bidirectional bending of the PAAc–PAAm bilayer actuator. As shown in Figure 3a, when the bilayer actuator is soaked in a relatively low pH solution (pH = 2), the PAAm layer (yellow) swells to a higher extent so that the bilayer hydrogel bends toward the PAAc layer (blue). Then, the pH level of the solution is tuned to 8. The bilayer actuator gradually bends toward the PAAm layer (yellow) due to the higher swelling ratio of the PAAc layer with ionized carboxyl groups in a high pH solution. Further changing the pH level to 2 makes the bilayer actuator bend to the PAAc side again. As a result, under the binary cooperation between the PAAm hydrogel layer and the PAAc layer, the bending direction of the PAAc–PAAm actuator could be regulated in different solution systems just by adjusting the pH value. Moreover, by alternately turning the pH, the PAAc–PAAm bilayer actuator achieves reversible deformation more than 20 times.

Just like the fiber architecture found in elephant trunk, various programmable motions (e.g., bending, twisting, and rolling) of the bilayer actuator can be achieved by exploiting the anisotropic local deformation induced by an external driving stimulus.<sup>31</sup> To implement the differential deformation design concept, an array of parallel elastomer stripes (VHB, very high bond tape) are set on one surface of the hydrogel layer. As shown in Figures 3b and S7, fiber architectures with the angles (0, 45, and 90°) of the stiff stripes relative to the long edge of the actuator are analogous to those of the biological counterpart. In our design, the multimaterial architecture leads to anisotropic strain upon stimulus. Understanding the motion achieved by the soft actuators is crucial for their design, programming, and successful operation in applications. To provide guidance on the design of fiber configuration in the hydrogel actuator to achieve the desired deformation, we conduct finite-element simulations using the ABAQUS software package to calculate the deformation of the pH-responsive hydrogel. We adopt the thermal expansion method to simulate the swelling of hydrogel. For the two different hydrogels, two distinct expansion coefficients are applied, with the larger expansion coefficient corresponding to

the hydrogel layer that undergoes larger deformation. Due to the large deformation of both hydrogel and VHB, we choose Neo-Hookean constitutive model. The element type is C3D8RH, with both the reduced integration and hourglass control technique adopted to ensure accuracy. We carried out three calculation cases, with the angles between VHB fibers and hydrogel matrix of 0, 45, and 90° (Figure 3c). The computational deformation patterns are qualitatively consistent with the experimental results (Figure 3d). When the hydrogel bilayer actuator swells in a solution with a certain pH, the elastomer stripe with a higher modulus<sup>32</sup> will constrain the deformation of the hydrogel in its vicinity. The region near the stripe swells lightly, while the region far away swells extensively. As a result, the hydrogel bilayer actuator bends approximately perpendicularly to the stripes and realizes the pH-triggered bending, twisting, and rolling.

**Lipophilic Payload Releases Simulation.** We evaluated the feasibility of the lipophilic drug release in vitro using a dual pH-responsive hydrogel actuator-controlled capsule. To simulate the real human environment, we chose pH values of 2, 6, and 8. At pH 6, the bilayer actuator reaches an equilibrium that the PAAc hydrogel swells to the same extent as the PAAm hydrogel swells. For the ease of observation and analysis, we amplified the functional capsule (a polyethylene hollow sphere with a diameter of 6 cm) in this in vitro experiment (Figure 4a). The capsule has a small square hole on its belly ( $1 \times 1 \text{ cm}^2$ ) to allow the lipophilic drugs to flow out. The dual pH-responsive hydrogel bilayer actuator ( $3 \times 2 \text{ cm}^2$ ) was used to cover the small hole as a capsule switch. The upper edge of the actuator was firmly fixed to the capsule, but the rest boundaries weakly adhered to the surface of the capsule using PVA (poly(vinyl alcohol)) glue. PVA glue can be quickly debonded in aqueous solution, and the debonding time can be controlled by the thickness of the coating. Here, the debonding time is roughly controlled around 5 min. The capsule was sealed well before the experiment. A dye solution with 0.5 g of carotenoid as a representative lipophilic drug was injected into the capsule. After these steps, we soaked these capsules in different aqueous solutions with different pH values (2, 6, and

8). At predetermined time intervals, 3 mL of each solution was withdrawn and spectro-photometrically analyzed (UV–vis spectroscopy) at 450 nm for carotenoid. Figure 4b shows that after being soaked in an aqueous solution with a pH of 2 or 6 for 20 min, the capsule switch was still closed, and it is difficult to see the seepage of the dye solution. Although the PVA glue is debonded, there is not enough strength to overcome the effect of water pressure. The dye will still be enclosed in the capsule with a weak penetration. It means that the drug can be well protected in the capsule before it is released, despite being in a low pH environment like gastric juice. However, upon being immersed in the aqueous solution of pH 8 for the first 10 min, the actuator gradually swells, partly detaches from the capsule, and then bends around its fixed upper edge (Figure 4b). Immediately after the capsule switch was opened, both the dye solution and carotenoid were released. The solution turned red quickly and the amount of the carotenoid in the solution increased fast. The concentration of released carotenoids versus time is plotted in Figure 4c. Within the first 5 min, the capsule switches did not open in all solutions, and carotenoids were barely released. After 10 min, carotenoids were initially released at a very high rate due to the opening of the capsule switch in the solution of pH 8. Within 2 h, more than 60% of carotenoids were released. For capsule switches in solutions of pH 2 and 6, small amounts of carotenoids were released from the capsule even after soaking for 6 h, indicating that the capsule switch works well and can achieve the efficient release of lipophilic drugs. We know that drugs sometimes need to be released under acidic conditions (such as stomach medicines). To meet the needs of these conditions, we can just turn over the bilayer hydrogel actuator and change the mounting direction. As a result, the PAAm hydrogel become the bottom layer and the PAAc hydrogel become the upper layer (Figure S8). Then, the capsule switch opens in the acidic solution (pH = 2). Therefore, the dual pH-response property brings convenience to the design of the capsule. One actuator can meet the needs of two different conditions.

## CONCLUSIONS

In summary, we propose an actuator-controlled drug release system for lipophilic drugs based on a dual pH-responsive hydrogel actuator. This hydrogel actuator can act as a capsule switch that releases drugs in a certain basic or acidic environment. We discussed the shape transformation of the bilayer actuator in aqueous solutions and achieved the bidirectional bending. Besides, various programmable motions of the bilayer actuator can be realized by incorporating an array of parallel elastomer stripes on one side of the hydrogel bilayer. Moreover, we conducted in vitro lipophilic drug release test and verified the feasibility of this drug release method. This dual pH-responsive actuator-controlled drug release system can release hydrophilic or lipophilic drugs based on the pH value of the environment and prevent the degradation, metabolism, and excretion of drugs before release. The actuator-controlled drug release method may shed light on more possibilities for various drug delivery systems.

## ASSOCIATED CONTENT

### Supporting Information

The Supporting Information is available free of charge at <https://pubs.acs.org/doi/10.1021/acsami.9b21713>.

Tough bonding of the hydrogel layers; pH-dependent ionization of basic functional groups on hydrogels chains responsible for swelling (Figure S1); preparation of bilayer hydrogels (Figure S2); covalent bonds formed between two hydrogel networks (Figure S3); 90 degree peeling test (Figure S4); the force–displacement curve of the peeling test for the PAAm–PAAc hydrogel bilayer (Figure S5); mechanical properties of pure PAAm hydrogel and PAAc hydrogel (Figure S6); and experimental design of the actuators with VHB stripes glued on one side (Figure S7) (PDF)  
90-degree peeling test (Movie S1) (MP4)  
Bidirectional bending can be achieved by adjusting the pH value of the solution (Movie S2) (MP4)

## AUTHOR INFORMATION

### Corresponding Authors

**Guodong Nian** – State Key Laboratory of Fluid Power & Mechatronic System, Key Laboratory of Soft Machines and Smart Devices of Zhejiang Province, Center for X-Mechanics, and Department of Engineering Mechanics, Zhejiang University, Hangzhou 310027, China; Email: [gnian@zju.edu.cn](mailto:gnian@zju.edu.cn)

**Shaoxing Qu** – State Key Laboratory of Fluid Power & Mechatronic System, Key Laboratory of Soft Machines and Smart Devices of Zhejiang Province, Center for X-Mechanics, and Department of Engineering Mechanics, Zhejiang University, Hangzhou 310027, China; [orcid.org/0000-0002-1217-4644](https://orcid.org/0000-0002-1217-4644); Email: [squ@zju.edu.cn](mailto:squ@zju.edu.cn)

### Authors

**Zilong Han** – State Key Laboratory of Fluid Power & Mechatronic System, Key Laboratory of Soft Machines and Smart Devices of Zhejiang Province, Center for X-Mechanics, and Department of Engineering Mechanics, Zhejiang University, Hangzhou 310027, China

**Peng Wang** – State Key Laboratory of Fluid Power & Mechatronic System, Key Laboratory of Soft Machines and Smart Devices of Zhejiang Province, Center for X-Mechanics, and Department of Engineering Mechanics, Zhejiang University, Hangzhou 310027, China

**Guoyong Mao** – State Key Laboratory of Fluid Power & Mechatronic System, Key Laboratory of Soft Machines and Smart Devices of Zhejiang Province, Center for X-Mechanics, and Department of Engineering Mechanics, Zhejiang University, Hangzhou 310027, China

**Tenghao Yin** – State Key Laboratory of Fluid Power & Mechatronic System, Key Laboratory of Soft Machines and Smart Devices of Zhejiang Province, Center for X-Mechanics, and Department of Engineering Mechanics, Zhejiang University, Hangzhou 310027, China

**Danming Zhong** – State Key Laboratory of Fluid Power & Mechatronic System, Key Laboratory of Soft Machines and Smart Devices of Zhejiang Province, Center for X-Mechanics, and Department of Engineering Mechanics, Zhejiang University, Hangzhou 310027, China

**Burebi Yiming** – State Key Laboratory of Fluid Power & Mechatronic System, Key Laboratory of Soft Machines and Smart Devices of Zhejiang Province, Center for X-Mechanics, and Department of Engineering Mechanics, Zhejiang University, Hangzhou 310027, China

**Xiaocheng Hu** – State Key Laboratory of Fluid Power & Mechatronic System, Key Laboratory of Soft Machines and Smart Devices of Zhejiang Province, Center for X-Mechanics,

and Department of Engineering Mechanics, Zhejiang University, Hangzhou 310027, China

**Zheng Jia** – State Key Laboratory of Fluid Power & Mechatronic System, Key Laboratory of Soft Machines and Smart Devices of Zhejiang Province, Center for X-Mechanics, and Department of Engineering Mechanics, Zhejiang University, Hangzhou 310027, China; [orcid.org/0000-0001-8459-515X](https://orcid.org/0000-0001-8459-515X)

**Wei Yang** – State Key Laboratory of Fluid Power & Mechatronic System, Key Laboratory of Soft Machines and Smart Devices of Zhejiang Province, Center for X-Mechanics, and Department of Engineering Mechanics, Zhejiang University, Hangzhou 310027, China

Complete contact information is available at:  
<https://pubs.acs.org/10.1021/acsami.9b21713>

### Author Contributions

S.Q., G.N., and W.Y. guided the entire work and provided useful suggestions. Z.H. did the experiments. P.W. helped to design the experiments. G.M., T.Y., D.Z., and B.Y. provided help in the data processing. All authors discussed and analyzed the results.

### Notes

The authors declare no competing financial interest.

## ACKNOWLEDGMENTS

This work is supported by the National Natural Science Foundation of China (Nos. 11525210, 11621062, and 91748209) and the Fundamental Research Funds for the Central Universities.

## REFERENCES

- (1) Li, J.; Mooney, D. J. Designing Hydrogels for Controlled Drug Delivery. *Nat. Rev. Mater.* **2016**, *1*, 16071–16087.
- (2) Fenton, O. S.; Olafson, K. N.; Pillai, P. S.; Mitchell, M. J.; Langer, R. Advances in Biomaterials for Drug Delivery. *Adv. Mater.* **2018**, *30*, 1705328–1705356.
- (3) Gong, C.; Lu, C.; Li, B.; Shan, M.; Wu, G. Injectable Dopamine-Modified Poly(Alpha,Beta-Aspartic Acid) Nanocomposite Hydrogel as Bioadhesive Drug Delivery System. *J. Biomed. Mater. Res., Part A* **2017**, *105*, 1000–1008.
- (4) Sengupta, P.; Chatterjee, B. Potential and Future Scope of Nanoemulgel Formulation for Topical Delivery of Lipophilic Drugs. *Int. J. Pharm.* **2017**, *526*, 353–365.
- (5) Gupta, S.; Kesarla, R.; Omri, A. Formulation Strategies to Improve the Advances in Engineering Hydrogels Bioavailability of Poorly Absorbed Drugs with Special Emphasis on Self-Emulsifying Systems. *ISRN Pharmaceutics* **2013**, *2013*, 848043–848059.
- (6) Lipinski, C. A. Drug-Like Properties and the Causes of Poor Solubility and Poor Permeability. *J. Pharmacol. Toxicol. Methods* **2000**, *44*, 235–249.
- (7) Allen, T. M.; Cullis, P. R. Drug Delivery Systems: Entering the Mainstream. *Science* **2004**, *303*, 1818–1822.
- (8) Zhang, Z.; Shi, L.; Wu, C.; Su, Y.; Qian, J.; Deng, H.; Zhu, X. Construction of a Supramolecular Drug–Drug Delivery System for Non-Small-Cell Lung Cancer Therapy. *ACS Appl. Mater. Interfaces* **2017**, *9*, 29505–29514.
- (9) Zhang, F.; Fan, J.; Zhang, P.; Liu, M.; Meng, J.; Jiang, L.; Wang, S. A Monolithic Hydro/Organo Macro Copolymer Actuator Synthesized Via Interfacial Copolymerization. *NPG Asia Mater.* **2017**, *9*, No. e380.
- (10) Liu, L.; Ghaemi, A.; Gekle, S.; Agarwal, S. One-Component Dual Actuation: Poly (Nipam) Can Actuate to Stable 3d Forms with Reversible Size Change. *Adv. Mater.* **2016**, *28*, 9792–9796.

(11) Ma, C.; Le, X.; Tang, X.; He, J.; Xiao, P.; Zheng, J.; Xiao, H.; Lu, W.; Zhang, J.; Huang, Y.; Chen, T. A Multiresponsive Anisotropic Hydrogel with Macroscopic 3d Complex Deformations. *Adv. Funct. Mater.* **2016**, *26*, 8670–8676.

(12) Zhang, Y. S.; Khademhosseini, A. Advances in Engineering Hydrogels. *Science* **2017**, *356*, eaaf3627.

(13) Van Opdenbosch, D.; Fritz-Popovski, G.; Wagermaier, W.; Paris, O.; Zollfrank, C. Moisture-Driven Ceramic Bilayer Actuators from a Biotemplating Approach. *Adv. Mater.* **2016**, *28*, 5235–5240.

(14) Yuk, H.; Lin, S.; Ma, C.; Takaffoli, M.; Fang, N. X.; Zhao, X. Hydraulic Hydrogel Actuators and Robots Optically and Sonically Camouflaged in Water. *Nat. Commun.* **2017**, *8*, No. 14230.

(15) Xue, B.; Qin, M.; Wang, T.; Wu, J.; Luo, D.; Jiang, Q.; Li, Y.; Cao, Y.; Wang, W. Electrically Controllable Actuators Based on Supramolecular Peptide Hydrogels. *Adv. Funct. Mater.* **2016**, *26*, 9053–9062.

(16) Zheng, J.; Xiao, P.; Le, X.; Lu, W.; Théato, P.; Ma, C.; Du, B.; Zhang, J.; Huang, Y.; Chen, T. Mimosa Inspired Bilayer Hydrogel Actuator Functioning in Multi-Environments. *J. Mater. Chem. C* **2018**, *6*, 1320–1327.

(17) Wang, X.; Jiao, N.; Tung, S.; Liu, L. Photoresponsive Graphene Composite Bilayer Actuator for Soft Robots. *ACS Appl. Mater. Interfaces* **2019**, *11*, 30290–30299.

(18) Haganan, D. E.; Leist, S.; Zhou, J.; Ji, H.-F. Photoactivated Polymeric Bilayer Actuators Fabricated Via 3d Printing. *ACS Appl. Mater. Interfaces* **2018**, *10*, 27308–27315.

(19) Hua, L.; Xie, M.; Jian, Y.; Wu, B.; Chen, C.; Zhao, C. Multiple-Responsive and Amphibious Hydrogel Actuator Based on Asymmetric Ucst-Type Volume Phase Transition. *ACS Appl. Mater. Interfaces* **2019**, *11*, 43641–43648.

(20) Kim, D.; Kim, H.; Lee, E.; Jin, K. S.; Yoon, J. Programmable Volume Phase Transition of Hydrogels Achieved by Large Thermal Hysteresis for Static-Motion Bilayer Actuators. *Chem. Mater.* **2016**, *28*, 8807–8814.

(21) Guo, Q.; Dai, E.; Han, X.; Xie, S.; Chao, E.; Chen, Z. Fast Nastic Motion of Plants and Bioinspired Structures. *J. R. Soc., Interface* **2015**, *12*, 20150598–20150611.

(22) Scorza, L. C. T.; Dornelas, M. C. Plants on the Move: Towards Common Mechanisms Governing Mechanically-Induced Plant Movements. *Plant Signaling Behav.* **2011**, *6*, 1979–1986.

(23) Liu, Z.; Calvert, P. Multilayer Hydrogels as Muscle-Like Actuators. *Adv. Mater.* **2000**, *12*, 288–291.

(24) Rizwan, M.; Yahya, R.; Hassan, A.; Yar, M.; Azzahari, A. D.; Selvanathan, V.; Sonsudin, F.; Abouloula, C. N. pH Sensitive Hydrogels in Drug Delivery: Brief History, Properties, Swelling, and Release Mechanism, Material Selection and Applications. *Polymers* **2017**, *9*, 137.

(25) Li, G.; Zhang, G.; Sun, R.; Wong, C.-P. Dually Ph-Responsive Polyelectrolyte Complex Hydrogel Composed of Polyacrylic Acid and Poly (2-(Dimethylamino) Ethyl Methacrylate). *Polymer* **2016**, *107*, 332–340.

(26) Rizwan, M.; Yahya, R.; Hassan, A.; Yar, M.; Azzahari, A.; Selvanathan, V.; Sonsudin, F.; Abouloula, C. Ph Sensitive Hydrogels in Drug Delivery: Brief History, Properties, Swelling, and Release Mechanism, Material Selection and Applications. *Polymers* **2017**, *9*, 137–173.

(27) Liu, Q.; Nian, G.; Yang, C.; Qu, S.; Suo, Z. Bonding Dissimilar Polymer Networks in Various Manufacturing Processes. *Nat. Commun.* **2018**, *9*, No. 846.

(28) Liu, S.; Boatti, E.; Bertoldi, K.; Kramer-Bottiglio, R. Stimuli-Induced Bi-Directional Hydrogel Unimorph Actuators. *Extreme Mech. Lett.* **2018**, *21*, 35–43.

(29) Kelby, T. S.; Wang, M.; Huck, W. T. S. Controlled Folding of 2d Au-Polymer Brush Composites into 3d Microstructures. *Adv. Funct. Mater.* **2011**, *21*, 652–657.

(30) Timoshenko, S. Analysis of Bi-Metal Thermostats. *J. Opt. Soc. Am.* **1925**, *11*, 233–255.

(31) Trivedi, D.; Rahn, C. D.; Kier, W. M.; Walker, I. D. Soft Robotics: Biological Inspiration, State of the Art, and Future Research. *Appl. Bionics Biomech.* **2008**, *5*, 99–117.

(32) Bozlar, M.; Punckt, C.; Korkut, S.; Zhu, J.; Chiang Foo, C.; Suo, Z.; Aksay, I. A. Dielectric Elastomer Actuators with Elastomeric Electrodes. *Appl. Phys. Lett.* **2012**, *101*, 091907–091912.

#### ■ NOTE ADDED AFTER ASAP PUBLICATION

Due to a production error, this paper was published on the Web on February 25, 2020, with author surname Yang incorrectly spelled as Yangph. The corrected version was reposted on February 26, 2020.